

Evaluation of Fluidic Pitch Links for Rotor Hub Vibration Controls

Jianhua Zhang
Email: jxz19@psu.edu

Lloyd H. Scarborough, III
Email: lloydhs3@gmail.com

Edward C. Smith
Email: ecs5@psu.edu

Christopher D. Rahn
Email: CDRahn@psu.edu

Department of Aerospace Engineering Department of Mechanical Engineering
The Pennsylvania State University, University Park, PA 16802, USA

Mark R. Jolly
Email: mark_jolly@lord.com

Lord Corporation, 110 Lord Drive, Cary, NC, 27511, USA

ABSTARCT

Researchers have been exploring the potential for fluidic pitch links to replace traditional rigid pitch links for rotorcraft vibration reduction. Previous studies showed that the hub vibratory loads of a medium-sized helicopter with an articulated rotor system in high speed flight condition could be affected by tailoring the fluidic pitch link impedance. The current research is intended to advance and expand studies of the fluidic pitch link concept. A free wake model is implemented in rotor aeroelastic modeling. The fluidic pitch links have been examined at low forward speed for the vehicle, the results show that they can achieve average 39% vibration reduction at advance ratio 0.15. Fluidic pitch links are also be evaluated on a light helicopter with a hingeless rotor system. Parametric studies of fluidic pitch link properties are conducted, and their effect on rotor hub vibratory loads is evaluated at both low and high forward speeds for its off-design performance. The results indicate that fluidic pitch links work very well at advance ratio of 0.30, and can reduce hub loads by average 45%. The fluidic pitch links are also compared with the active individual blade pitch controls. The simulation results show their performances, in terms of rotor hub vibration reductions are comparable.

INTRODUCTION

It is known that controlled higher harmonic pitching motion of rotor blades can lead to rotor vibratory load reduction and performance improvement. Higher harmonic pitch controls may be superimposed on the rotor collective and cyclic inputs using the swashplate, an approach known as Higher Harmonic Control (HHC). The effectiveness of HHC was validated both by simulations ^[1] and tests ^[2]. Individual Blade control (IBC), which usually was achieved by hydraulic actuators that replaced rigid pitch links, has also been investigated. IBC effects on rotor vibration and noise reduction were demonstrated experimentally and theoretically ^[3, 4]. Adoption of active IBC systems involves trades between system performance, and reliability, complexity, and cost concerns. Comparing to HHC and IBC, which excite the blade at the blade root, active Trailing Edge Flaps (TEF) can elastically twist the blade by the additional forces and moments generated near the blade tip. Various studies of active TEF have found that TEF can achieve more

vibration reduction with less control effort ^[5-7] compared to HHC or IBC.

Passive approaches of blade pitching controls have also been investigated, since they have potential to be simple and lower cost and more reliable. Milgram et al. replaced the rigid pitch link with a spring/damper element to shift the natural frequency from the excitation frequency to reduce vibratory hub loads ^[8]. Han et al. proposed replacing the rigid pitch links with fluidlastic isolators to reduce pitch-link loads ^[9], the simulation results showed that the fluidlastic isolators can reduce the 4/rev pitch link load by more than 90% in high forward flight with small variations in the other harmonic loads, however, their impact on rotor vibratory hub loads was not examined.

Recently, Scarborough et al. ^[10] demonstrated that fluidic pitch links (FPL) could be employed to tailor the blade pitching response by altering the blade root torsional impedance (Figure 1). The impedance of a mechanical system relates an

applied force to the resulting velocity of the system. Jolly and Margolis presented a framework for describing a mechanical system in terms of an impedance matrix. If the eigenvalues of the impedance matrix are positive, then the impedance can be realized by a passive mechanical system [11]. The parametric studies of FPL were conducted in Reference 10 using UH-60 type helicopter model at high advance ratio of 0.3. The simulation results showed that all six vibratory hub loads may be influenced by tailoring the impedance of the FPL.

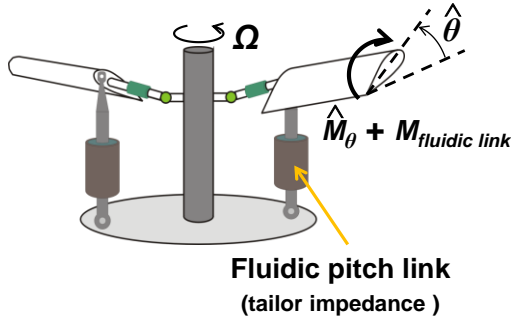


Figure 1. Impedance tailoring of fluidic pitch link

MOTIVATIONS AND OBJECTIVES

The current research is to address some deficiencies in rotor modeling, and to expand the scope of the FPL studies conducted in Reference 10. It is expected that the wake has significant influences on the accuracy of rotor vibratory load prediction, especially at the low forward speed. Therefore, a free wake model is implemented in the rotor aeroelastic modeling, such that the studies can be carried out at the lower forward speed as well. Then, the effect of the FPL on rotor vibratory loads is examined under the influence of the free wake. Parametric studies of the FPL are conducted at both low and high speed flight. An off-design situation is investigated, in which the optimal FPL configuration suitable for the high speed flight is examined at the low speed flight. Besides the articulated UH-60 type rotor model, the FPL is applied on hingeless BO-105 type helicopter. Finally, the effectiveness of this passive FPL device is compared to the active individual blade pitch controls.

ANALYTICAL MODEL

The FPL model formulated in Reference 10 is used in the current study, and briefly described in this section. The rotor model including the free wake model developed in Reference 6 is integrated with the FPL model. The details of how active IBC is implemented are also provided in this section.

Fluidic Pitch Link Modeling

A FPL model shown in Figure 2 was developed in Reference 10. The pitch link has a piston of area A and mass m that is sealed and elastically restrained by an elastomer with damping c and stiffness k . The piston moves with displacement $x(t)$ in response to $F(t)$. For a given pitch-horn length, l_{ph} , $F(t)$ and $x(t)$ are related to the blade-root pitching moment, $M_\theta(t)$, and the blade-root elastic twist, $\theta_r(t)$, by Equation 1 and 2 respectively.

$$(1) \quad F = \frac{M_\theta}{l_{ph}}$$

$$(2) \quad x = l_{ph}\theta_r$$

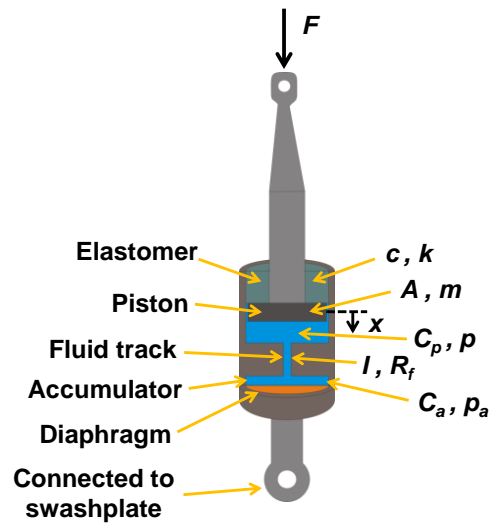


Figure 2. Schematic of a fluidic pitch link

The primary chamber of the pitch link has capacitance C_p and pressure, $p(t)$, generated by the motion of the piston as it forces fluid volume $V(t)$ into the fluid track. The fluid track has area a and length L . The fluid in the track has density ρ and the lumped inertia I in the track is defined as,

$$(3) \quad I = \frac{\rho L}{a}$$

The resistance to fluid flow, R_f , of the fluid track is assumed to be constant. The fluid track terminates in an accumulator with capacitance C_a and pressure $p_a(t)$.

Summing the forces on the piston gives the first equation of motion

$$(4) \quad m\ddot{x} + c\dot{x} + \left(k + \frac{A^2}{C_p}\right)x - \frac{A}{C_p}V = F$$

The mechanical-fluidic coupling equation is

$$(5) \quad V = Ax - C_p P$$

The equation for the fluid flow through the fluid track is

$$(6) \quad p - p_a = I\ddot{V} + R_f \dot{V}$$

Fluid flow into, and out of, the accumulator dictates the change in accumulator pressure

$$(7) \quad \dot{p}_a = \frac{1}{C_a} \dot{V}$$

Combining Equations 5-7 yields the second equation of motion

$$(8) \quad I\ddot{V} + R_f \dot{V} + \left(\frac{1}{C_a} + \frac{1}{C_p}\right)V - \frac{A}{C_p} x = 0$$

A rotor aeroelastic analysis developed in Reference 6 was adapted by including the fluidic pitch link model described above. It introduces one additional degree of freedom (fluid volume, V) to the rotor aeroelastic simulation, which is discussed in the following section.

Rotor aeroelastic modeling with a free wake

The rotor aeroelastic simulation is adapted from Reference 6. The helicopter is modeled as a single main rotor connected to a rigid fuselage. Each blade is assumed to undergo flap bending, lag bending and torsion deformations. The deformations are supposed to be of moderate magnitude and strains are assumed to be small. The continuous blade is discretized in finite elements with eleven degrees of freedom for each element. Hamilton's variational principle is used to derive the discretized nonlinear governing differential equations. The blade strain energy, kinetic energy and virtual work are numerically integrated over the blade elements to yield the elemental mass, damping and stiffness matrices as well as the constant and nonlinear force vectors.

A coupled propulsive trim procedure is used to solve for the blade steady responses in modal space via finite element method in time. The blade loads are calculated in the rotating frame by integrating all forces and moments acting on the blade along the blade radius. The blade root loads in the rotating frame are then transformed into the fixed frame to determine the vibratory hub loads. The hub vibratory loads consist of three shear forces: longitudinal force F_x , lateral force F_y , vertical force

F_z) and three moments: roll moment M_x , pitch moment M_y , torque M_z . The directions of these forces and moments are shown in Figure 3.

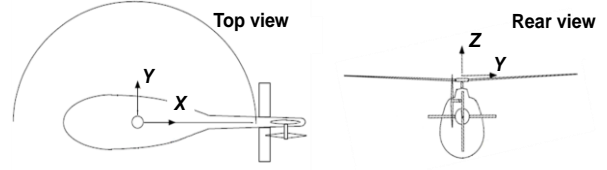


Figure 3. Coordinates for hub loads

Adding the fluidic pitch link model described above introduces one additional degree of freedom (fluid volume, V) to the rotor aeroelastic simulation. The root of the blade pitches elastically in addition to blade pitch control inputs. The mass, damping, and stiffness matrices are modified to include the fluidic pitch link contributions to the system. The introduction of the fluidic pitch link alters the response, which in turn, alters the blade root loads, and thus, the hub loads.

Aerodynamic loads acting on the blade are calculated using either quasi-steady blade element theory or a table lookup method. In the present study, a set of tables containing values for the lift, drag, and pitching moment coefficients as functions of both local airfoil sectional angle of attack and Mach number are used.

The free wake model used in this study was developed in Reference 12. It follows the free wake methodology initially developed by Bagai [13]. The wake is divided into near wake and far wake. The near wake consists of trailing vortices generated by the spanwise change in lift. The far wake is created by the trailing vortices rolling up outside of maximum load location into one tip vortex.

Active vibration controls using IBC

To evaluate the effectiveness of passive FPL, the active approach of IBC is also investigated in this study (Figure 4). The results of active vibration controls are compared with the results using the passive FPL method.

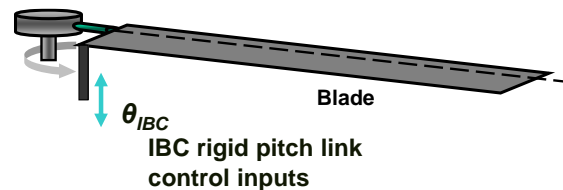


Figure 4. Active vibration controls using IBC

The IBC control is simulated using high harmonic root pitch controls. The active control actions (i.e. the root pitch control inputs of IBC) are

predicted based on an optimal control law. This optimal control law was originally developed in Reference 14, and is based on the minimization of the following quadratic objective function J ,

$$(9) \quad J = Z_n^T W_Z Z_n + \delta_n^T W_\delta \delta_n$$

where Z_n is hub vibratory load vector containing 4/rev sine and cosine harmonics at time step n for a four-bladed rotor (Equation 10); δ_n is active control input vector containing cosine and sine higher harmonics at time step n , typically 3, 4, 5/rev for a four-bladed rotor (Equation 11); W_Z and W_δ are the weighting matrices for vibration and control effort respectively, they can be varied to balance the targeted vibration reductions and required active control inputs.

$$(10) \quad Z_n = [F_{xc} \quad F_{xs} \quad F_{yc} \quad F_{ys} \quad F_{zc} \quad F_{zs} \\ M_{xc} \quad M_{xs} \quad M_{yc} \quad M_{ys} \quad M_{zc} \quad M_{zs}]^T$$

$$(11) \quad \delta_n = [\delta_{3c} \quad \delta_{3s} \quad \delta_{4c} \quad \delta_{4s} \quad \delta_{5c} \quad \delta_{5s}]$$

From Equation 11, the IBC rigid pitch control inputs as a function of azimuth can be written as,

$$(12) \quad \delta(\psi) = \sum_{i=3}^5 [\delta_{ic} \cos(i\psi) + \delta_{is} \sin(i\psi)]$$

In this study, the so-called “feedback form of global controller” [6] is implemented since the system is only moderately nonlinear. It is obtained by linearizing the system about current control inputs δ_{n-1} in the first order Taylor series expansion (Equation 13).

$$(13) \quad Z_n = Z_{n-1} + T_0(\delta_n - \delta_{n-1})$$

where T_0 is a gradient transfer matrix that represents the system response to control and relates the sine and cosine amplitudes of the control harmonics to the sine and cosine amplitudes of the vibration harmonics.

Substituting Equation 13 into the objective function (Equation 9)) and minimizing the objective function by solving Equation 14 yields the algorithm for calculating the optimal control input vector δ_n (Equation 15).

$$(14) \quad \frac{\partial J}{\partial \delta_n} = 0$$

$$(15) \quad \begin{aligned} \Delta \delta_n &= CZ_{n-1} - C_\delta \delta_{n-1} \\ \delta_n &= \delta_{n-1} + \Delta \delta_n \end{aligned}$$

where C and C_δ in Equation 15 are two matrices related to T_0 , W_Z , W_δ and Z_{n-1} . This controller (Equation 15) is in a closed-loop form where the control input during each control step is determined by feedback of the measured vibration levels as well as the control inputs of the previous step.

RESULTS AND DISCUSSION

Two helicopter models are investigated in this study. The first model is a medium weight, UH-60 type helicopter with an articulated rotor system, and the second model was a light weight BO-105 type helicopter with a hingeless rotor system. These models are meant to be representative of these helicopters, but they are simplified and do not exactly model all aspects of these vehicles. The terms “UH-60” and “BO-105” are used only to refer to these two types of helicopters in this paper.

Table 1. Rotor and blade properties

	BO-105	UH-60
Helicopter weight, W (lbs)	5,800	16,800
Hub type	Hingeless	Articulated
Number of Blade, N_b	4	4
Radius, R (ft)	16.2	26.8
Angular velocity, Ω (rad/sec.)	40.12	27.05
Airfoil	NACA 0015	SC 1095
Ref. Lift curve slope, a	5.73	5.73
Chord, (ft)	1.29	1.73
Solidity, σ	0.1	0.0822
Weight coefficient, C_W	0.007	0.006
Linear Twist, θ_{tw}	-8°	-8°
Lock Number, γ	6.34	6.53
Blade reference mass, m_0 (slug/ft)	0.1350	0.2357
Blade root attachment point	0.04R	0.04664R
Aerodynamic root cutout	0.1R	0.1429R
1 st flap frequency ($/\Omega$)	1.16	1.04
1 st lag frequency ($/\Omega$)	0.74	0.27
1 st torsion frequency ($/\Omega$)	3.55	4.50

The UH-60 and BO-105 helicopter models are investigated first to establish the baseline vibration levels with a free wake model at both a low and a high advance ratio. Then, parametric studies of the FPL model are conducted to evaluate the effectiveness of the FPL for hub vibratory load reduction. The active vibration controls using IBC are investigated and the results are compared to the FPL approach.

Analysis of Baseline Rotors

The baseline vibration analysis is conducted in this section. The vibratory hub loads generated in this section are used as the baseline values to evaluate the effectiveness of both passive FPL and the active IBC control approach for vibration reduction. The basic rotor and blade properties are listed in Table 1. The UH-60 type helicopter properties used in the study can be found in Reference 15, and BO-105 type helicopter data are from Reference 16.

The vibratory hub loads are evaluated at both advancing ratio of 0.15 and 0.30. These two flight speeds represent two different vibration problems. At low advance ratio, the major source of vibration is from the wake induced loading since the tip vortices remain very close to the disk plane. At high advance ratio, the prime source of vibration is due to the increased periodicity in aerodynamic loads; however, the influence of the wake effect can still be measurable.

The 4/rev vibratory hub loads for UH-60 and BO-105 at the advance ratio 0.15 are shown in Figure 5 and 6, respectively. Three hub shears (F_x , F_y , F_z) and three moments (M_x , M_y , M_z) are calculated with the free wake model and compared to the results using Drees linear inflow model. The significant differences of predicted vibratory hub loads show the importance of using the free wake model.

Studies of FPL for UH-60 Helicopter

To investigate the potential of the FPL to influence hub loads, parametric study of the FPL was conducted in Reference 10 for UH-60 helicopter at advance ratio of 0.30. Four of the fluidic pitch link parameters are varied. They are: accumulator capacitance (C_a), elastomer stiffness (k), inertance (I), and piston area (A). These parameters depend on fluidic pitch link geometry (piston diameter, accumulator volume, and fluid-track length) and material properties. The set of parameters which shows the best potential in Reference 10 is listed in Table 2.

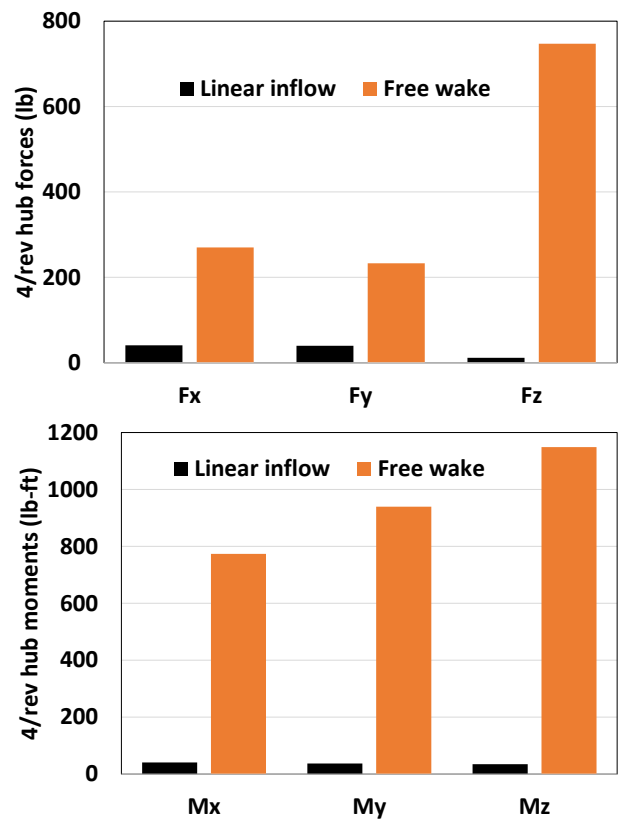


Figure 5 UH-60 vibratory hub loads at advance ratio 0.15

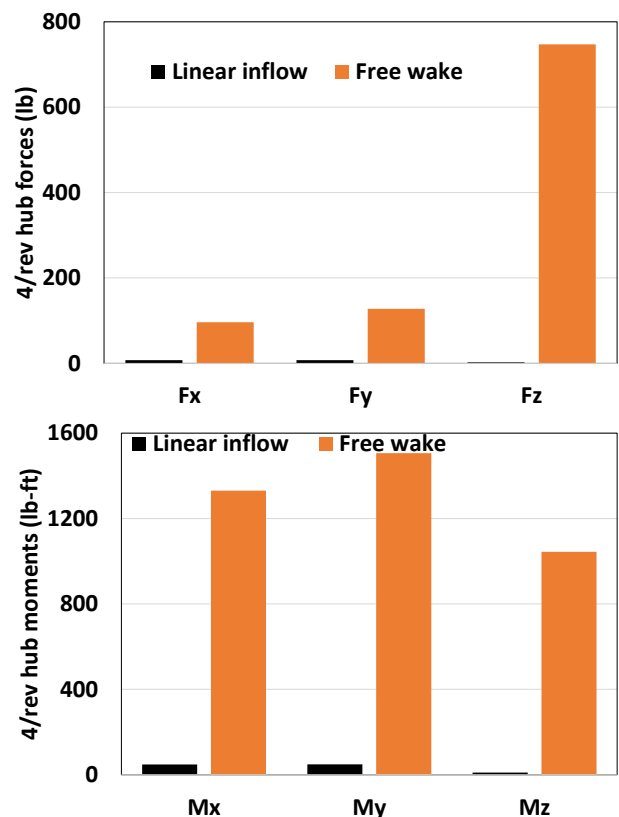


Figure 6. BO-105 vibratory hub loads at advance ratio 0.15

Table 2. FPL parameters

Description	UH-60	BO-105
Piston area, A (ft ²)	0.06	0.06
Piston mass, m (Slug)	0.03	0.025
Elastomer damping, c (lb.s/ft)	15.0	15.0
Elastomer stiffness, k (lb/ft)	45,000	40,000
Pitch link capacitance, C_p (ft ⁵ /lb)	2.0e-9	2.0e-9
Accumulator capacitance, C_a (ft ⁵ /lb)	2.0e-7	2.0e-7
Inertance, I (slug/ft ⁴)	4500	3500
Flow resistance, R_f (lb.s/ft ⁵)	5000	5000
Pitch horn length, l_{ph} (ft)	0.6	0.4

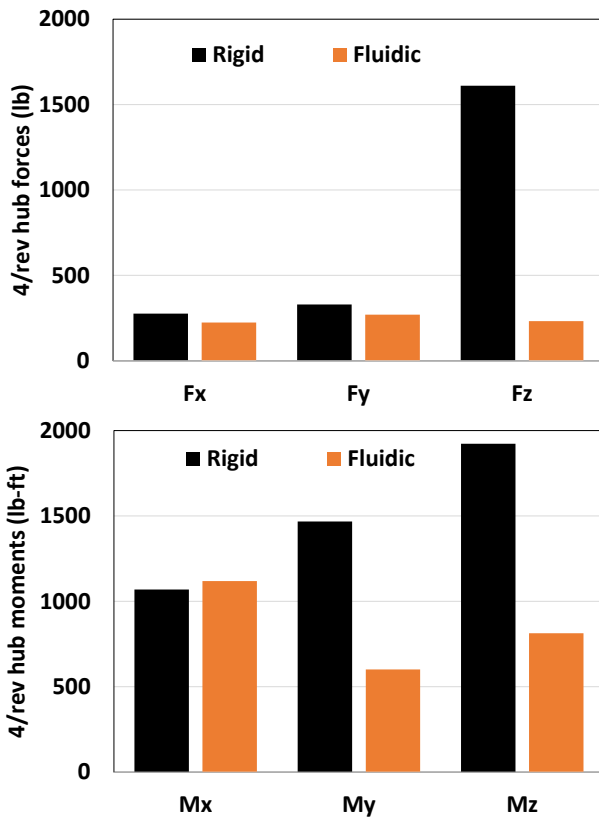


Figure 7. UH-60 hub vibratory load comparison at advance ratio 0.15

The results in Reference 10 indicated that FPL can influence all six hub vibratory components. Using the set of FPL parameters in Table 2, the simulation conducted in Reference 10 showed the significant reduction of hub inplane shear forces and pitching moment (about 50% reduction for F_x and 90% reduction for F_y , and 60% reduction for M_y), however, large increases of hub vertical shear (F_z) and roll moments (M_x) were also observed.

In this study, the FPL model developed in Reference 10 is investigated for its effectiveness at low flight speed of UH-60 helicopter (advance ratio 0.15). The rotor hub vibratory loads with the FPL are compared to the case with the rigid pitch link. The results showed in Figure 7, indicate that the FPL works quite well for hub vibration reduction at low forward flight speed; the rotor hub vertical force (F_z) and rotor roll moment (M_y) and torque (M_z) are significantly reduced, while only rotor roll moment (M_x) is slightly increased compared to the case with the rigid pitch link. Figure 8 shows the percentage reductions (positive values) or increases (negative values) of hub vibratory loads when the FPL is used compared to the rigid pitch link case at both high and low advance ratios of 0.30 and 0.15. Overall, the FPL has better performance in terms of hub load reduction at low advance ratio of 0.15 than at high advance ratio of 0.30. The average vibration reductions are about 39% at advance ratio of 0.15, about 17% at advance ratio of 0.30.

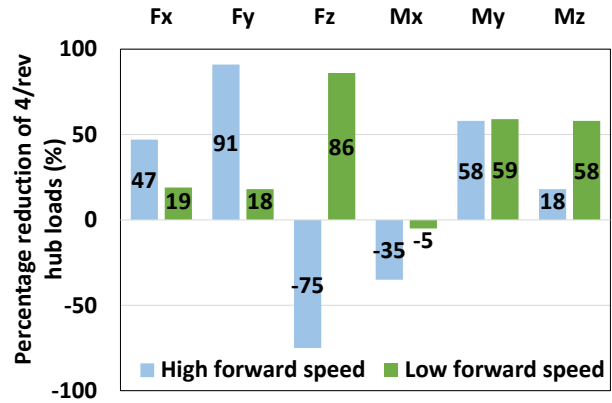


Figure 8. Percentage reduction of hub vibratory loads using the FPL at advance ratios 0.30 and 0.15 (Results at advance ratio 0.30 are from Reference 10)

The blade elastic torsion responses versus azimuth angle are shown in Figure 9. The tip response of the blade with the FPL have much larger amplitude compared to the tip response of the blade with the rigid pitch links. The root response of the blade with the FPL is also shown, and it differs from the blade tip response, indicating that the blade elastically twists due to the aerodynamic pitching moment.

The effect of the FPL on the higher-harmonic pitching motions of the blade is shown in Figure 10. The 2/rev, 3/rev, 4/rev and 5/rev components of blade tip responses are compared between the blade with the FPL and the blade with the rigid pitch links. It is observed that by using the FPL, the amplitudes of 2/rev and 5/rev responses increase, while the amplitudes of 3/rev and 4/rev decrease. These may due to the fact that replacing the rigid

pitch links with the FPL may lower the blade torsion stiffness. The original UH-60 with the rigid pitch links has the first torsion natural frequency about 4.5/rev; using the FPL reduces the first torsion natural frequency to about 2.1/rev and the second natural frequency about 4.8/rev. Additional parametric and design studies are being conducted for FPL designs with higher static stiffness (k). Torsional pitch-flap flutter analyses of rotors with the FPL is also underway. Frequency dependent inertia and coupling between root pitch and internal flow motion are unique to the FPL device.

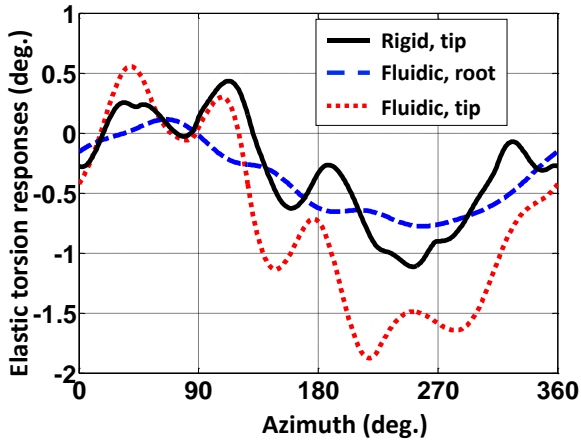


Figure 9. Blade elastic torsion responses at advance ratio 0.15

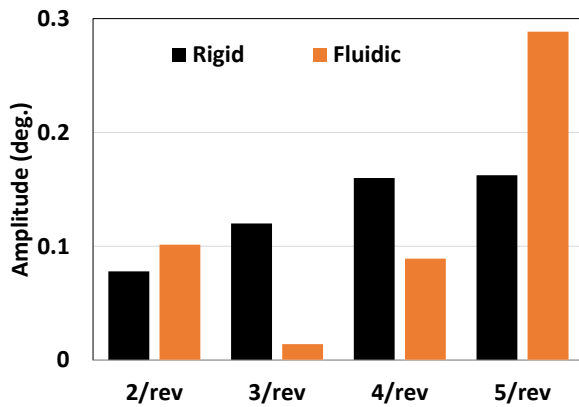


Figure 10. Amplitude of higher harmonic blade pitching motion at advance ratio 0.15

Parametric Studies of FPL for BO-105 Helicopter

The FPL model developed in Reference 10 for UH-60 helicopter is explored for hingeless rotor of BO-105 in this section. Parametric studies of the FPL model for BO-105 are conducted to find a FPL configuration that works for BO-105 rotor at advance ratio of 0.30. Seven parameters are investigated in the current study. Among them, inertia (I), piston mass (m), elastomer stiffness (k), accumulator capacitance (C_p) and piston area (A), are found to be of influences on rotor hub vibratory loads, while

elastomer damping (c) and flow resistance (R_f) have little effect. As examples, the sensitivity study results for the elastomer stiffness (k) and inertia (I) are shown in Figures 11 and 12, respectively. Three different values are assigned for k and I , the corresponding vibration levels are evaluated based on the percentage vibration reductions compared to the case using the rigid pitch link. The results indicate that these parameters has effect on all six vibratory components, and the rotor vertical shear is especially sensitive to the variation of these two parameters.

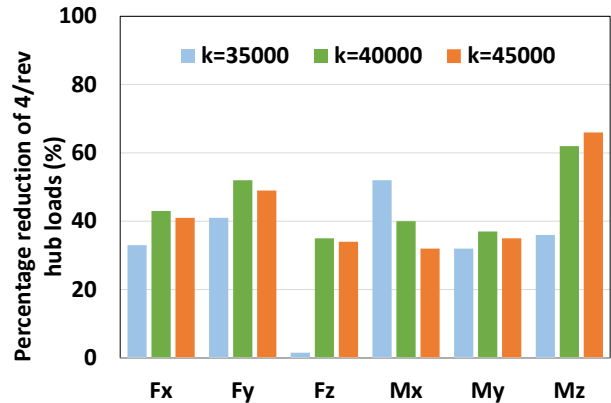


Figure 11. Parametric study of elastomer stiffness, k , at advance ratio 0.30

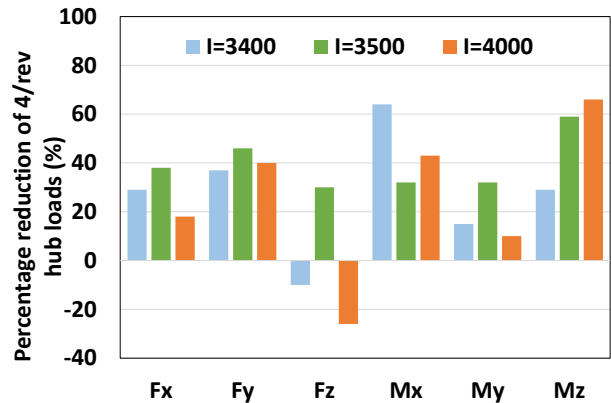


Figure 12. Parametric study of inertia, I , at advance ratio 0.30

Based on the parametric studies, a FPL design case is selected to show its effectiveness on rotor vibration reduction, and its parameters are shown in Table 2. Compared to the FPL configuration for UH-60 rotor, the values of three parameters of the FPL: the inertia (I), the elastomer stiffness (k) and piston mass (m), need to be modified for BO-105 rotor. The resulted hub vibratory load reductions are shown in Figure 13. Compared to the case with the rigid pitch links, average vibration reduction for all six vibratory components is about 45%. The blade elastic torsion responses are compared between the blade with the FPL and the blade with the rigid pitch links (Figure 14).

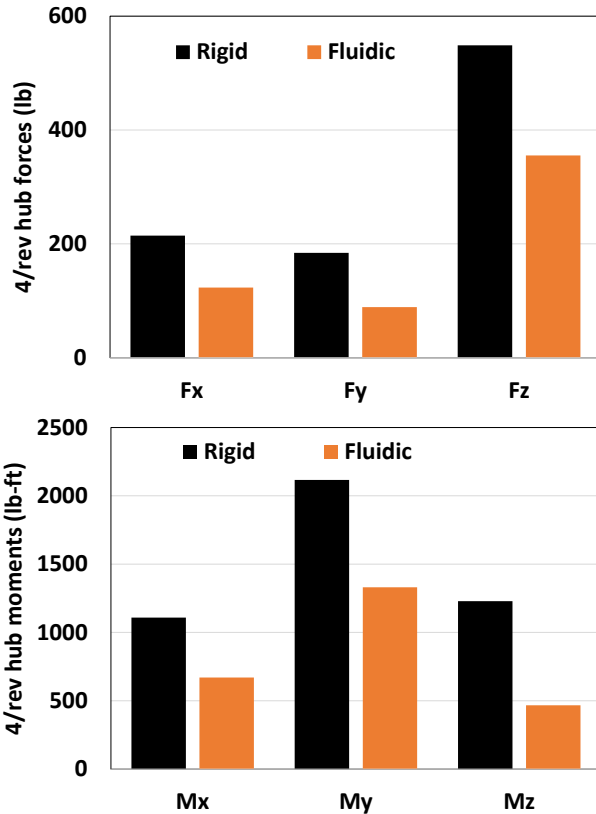


Figure 13. BO-105 hub vibratory load comparison at advance ratio 0.30

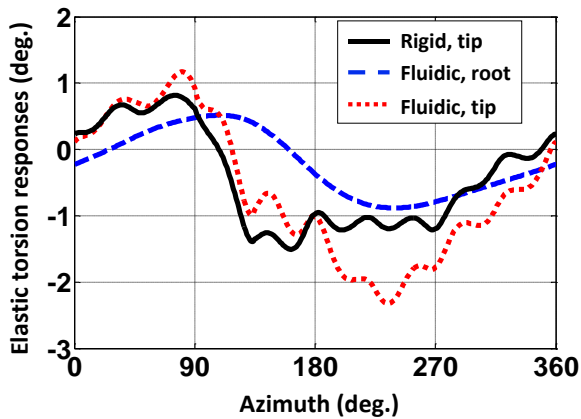


Figure 14. Blade elastic torsion responses at advance ratio 0.30

Parametric study is also conducted for the FPL at low advance ratio of 0.15. The study finds that the rotor vibratory hub loads are not sensitive to the variations of the FPL design parameters, indicating that the FPL does not influence the rotor blade torsion responses.

The FPL configuration targeted for high advance ratio of 0.30 is implemented at low advance ratio of 0.15, the effect of the FPL on rotor vibratory loads at low advance ratio is shown in Figure 15. Compared

to the results at advance ratio of 0.30, which has average reduction of 45%, the vibration reduction at advance ratio of 0.15 is negligible.

The blade tip torsion responses versus azimuth angle at advance ratio 0.15 are shown in Figure 16. The blade experiences much less higher-frequency oscillation at advance ratio 0.15 than at high advance ratio of 0.30 (Figure 14). The lack of torsion motion at low advance ratio is related to the airfoil shape for BO-105. In the current study, NACA 0012 data is implemented, and airfoil moment coefficients at low speed forward flight do not vary as much as at high advance ratio.

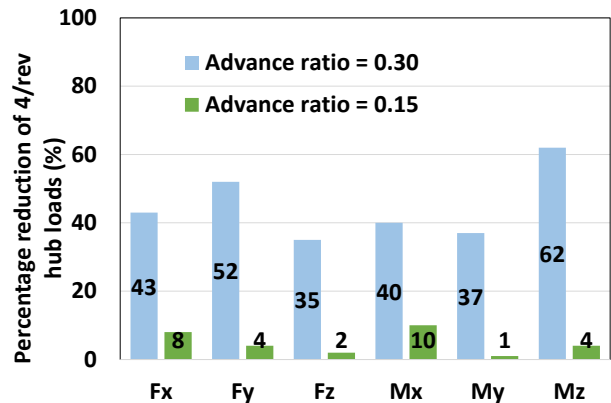


Figure 15. Comparison of vibration reduction at low advance ratio and at high advance ratio for BO-105

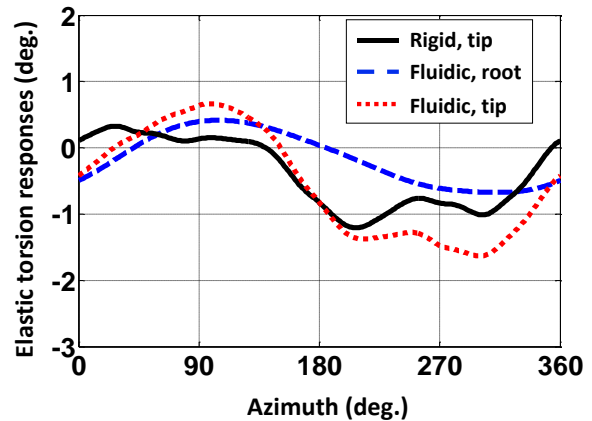


Figure 16. Blade elastic torsion responses at advance ratio 0.15

Comparison of the FPL with active vibration control approaches

To evaluate the effectiveness of the FPL for vibration reduction, the active approach of IBC is applied for BO-105 model. IBC excites the rotor blade at the root using the hydraulic actuation

system. For a four bladed rotor, 3, 4 and 5/rev high harmonic pitch control inputs are usually applied. Rotor 4/rev hub loads for both FPL and IBC are shown in Figure 17 for the case of advance ratio 0.30, overall vibration reductions compared to the baseline rigid pitch link configuration are similar, 45% using the FPL and 43% by IBC.

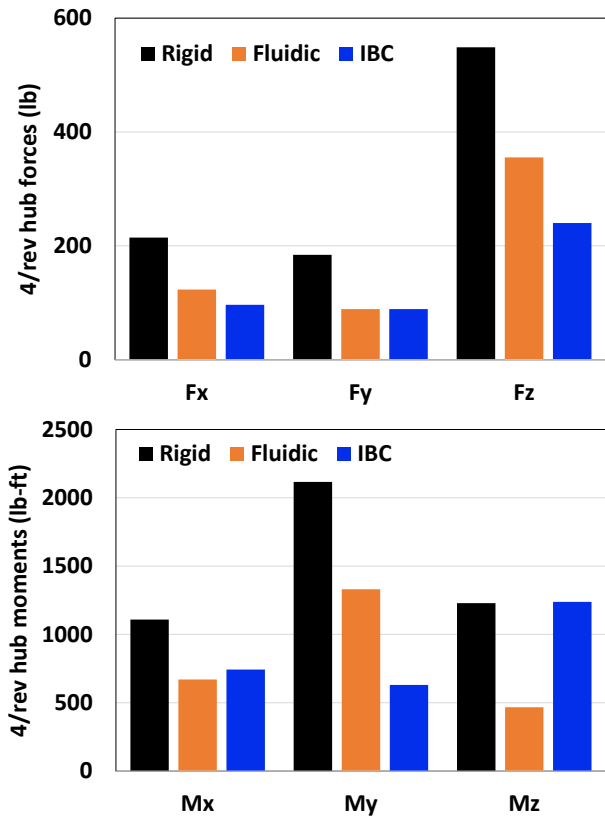


Figure 17. Comparison of vibratory hub loads at advance ratio 0.30 for BO-105

The comparison is also made at low advance ratio of 0.15 (Figure 18). Comparing to the FPL, which is not effective at low forward speed flight, the IBC active approach can significantly reduce the rotor vertical shear (F_z) and roll (M_x) and pitch (M_y) moments, however, moderate increases of longitudinal force (F_x) and rotor torque (M_z) are also observed.

The elastic torsion responses at the blade tip are shown in Figure 19 for IBC controls. High harmonic pitch motions of the blade are observed due to the IBC pitch control inputs. Compared to the blade tip elastic torsion response results of the FPL in Figures 14 and 16 for advance ratio 0.30 and 0.15 respectively, the amplitude of IBC blade pitch motions are much higher. The IBC root pitch controls are also shown in Figure 20 as described in Equation 12 as a function of rotor azimuth angles. The inputs comprise of 3, 4 and 5/rev root pitch

control components. By comparing the active IBC control inputs in Figure 20 to the output (the resulted blade tip responses in Figure 19), about 2° of the IBC control inputs generate about $5-7^\circ$ of the blade tip twist; ratio of the output to the input is about 3. Similar comparison can be made for the case with the FPL. The ratio between the blade tip twist and the blade root pitch motion is about 3 for the case of UH-60 (Figure 9), and about 2 for the case of BO-105 (Figure 14).

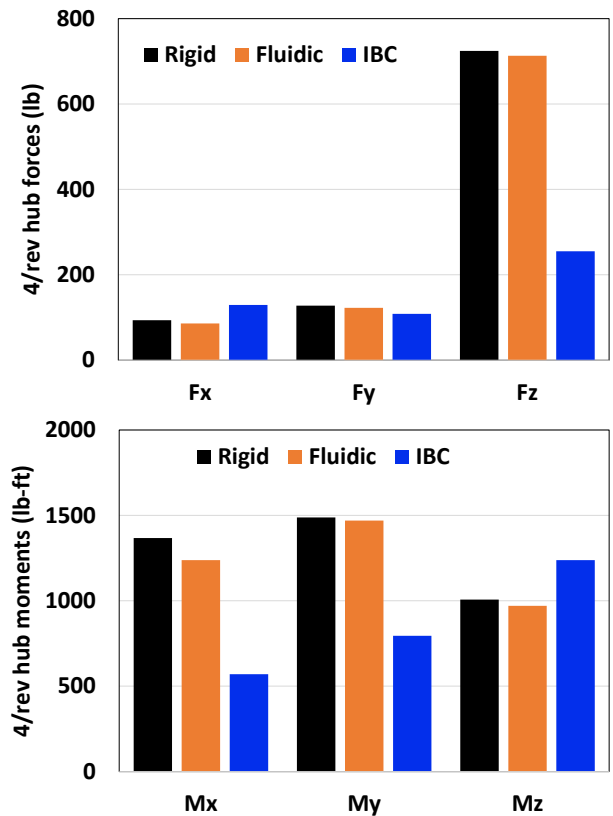


Figure 18. Comparison of vibratory hub loads at advance ratio 0.15 for BO-105

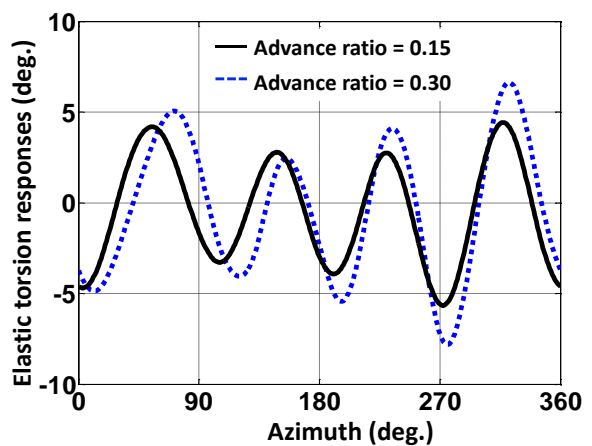


Figure 19. Blade tip elastic torsion responses using IBC

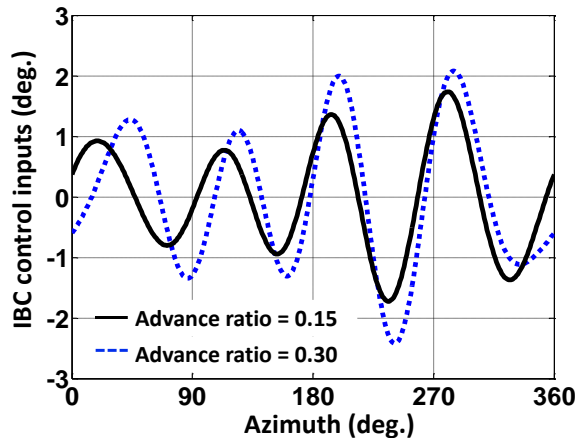


Figure 20. IBC root pitch control inputs

CONCLUSIONS

Fluidic pitch links have been explored to replace traditional rigid pitch links for their potential to reduce rotor vibratory hub loads. Two types of rotor: BO-105 hingeless and UH-60 articulated, are investigated with a free wake model. Parametric studies of the FPL have been conducted to examine the sensitivity of these parameters for rotor hub vibratory loads; the results are also compared to the active IBC control approach. The following conclusions can be made based on this study:

1. FPL has been examined at low forward speed for UH-60 helicopter with a free wake model, the results indicate that the FPL works better at the advance ratio of 0.15 than 0.30, which was investigated in Reference 10. The average vibration reduction for all six hub vibratory loads is about 39% for the case of advance ratio 0.15, twice as much as the reduction of 17% at the advance ratio 0.30.
2. Parametric study of the FPL for BO-105 rotor has been conducted. It has been found that the inertance, piston mass, elastomer stiffness, accumulator capacitance and piston area of the FPL, are of influences on rotor hub vibratory loads.
3. Based on the parametric study, a FPL model has been configured for BO-105 rotor, and applied at two rotor advance ratios: 0.15 and 0.30. The results show that the FPL works very well at advance ratio of 0.30, it can reduce hub loads by average 45%, while its effect at the advance ratio 0.15 is negligible.

4. The FPL approach is also compared to the active IBC controls. The results indicate that the FPL can perform as well as the IBC in terms of rotor hub vibration control at the advance ratio of 0.30.
5. The semi-active FPL proposed in Reference 10 needs to be explored to account for variation of flight speeds and maneuvering. For example, using valves, fluidic circuits with different fluid-track lengths, could be switched in based on the flight regime to improve the effectiveness of FPL at different flight conditions.
6. Blade airfoil characteristics, especially, the blade airfoil moment coefficient, may be important parameter for the performance of a rotor with the FPL. This may open the design space for rotor airfoils in the future, and is worth further study.

ACKNOWLEDGMENTS

The authors would like to express their appreciation for the financial support provided by LORD Corporation.

REFERENCES

1. Shaw Jr., J., "Higher Harmonic Blade Pitch Control for Helicopter Vibration Reduction: A Feasibility Study," *Aeroelastic and Structures Research Laboratory Rep. ASRL 150.1, AD702773*, Massachusetts Institute of Technology, Cambridge, MA, 1968.
2. McHugh, F. J. and Shaw, J., "Helicopter Vibration Reduction with Higher Harmonic Blade Pitch," *Third European Rotorcraft and Powered Lift Aircraft Forum*, Aix-en-Provence, France, September 7–9, 1977.
3. Jacklin, S., Blaas, A., Teves, D., and Kube, R., "Reduction of Helicopter BVI Noise, Vibration, and Power Consumption Through Individual Blade Control," *Proceedings of American Helicopter Society 51st Annual Forum*, Fort Worth, TX, May 9–11, 1995.
4. Yeo, H., Romander, E. A., and Norman, T. R., "Investigation of Rotor Performance and Loads of a UH-60A Individual Blade Control System," *Journal of the American Helicopter Society*, Vol. 56, (4), October 2011, pp.1–18.
5. Millott, T. A. and Friedmann, P. P., "Vibration Reduction in Helicopter Rotors Using an Actively Controlled Partial Span Trailing Edge Flap Located on the Blade," *NASA Contractor Reports*, Vol. 4611, 1994.

6. Zhang, J., Smith, E. C., and Wang, K. W., "Active-Passive Hybrid Optimization of Rotor Blades with Trailing Edge Flaps," *Journal of the American Helicopter Society*, Vol. 49, (1), January 2004, pp. 54–65.
7. Liu, L., Friedmann, P., Kim, I., and Bernstein, D., "Simultaneous Vibration Reduction and Performance Enhancement in Rotorcraft Using Actively Controlled Flaps," *Proceedings of American Helicopter Society 62nd Annual Forum*, Phoenix, AZ, May 9–11, 2006.
8. Milgram, J., Chopra, I., and Kottapalli, S., "Dynamically Tuned Blade Pitch Links for Vibration Reduction," *Proceedings of American Helicopter Society 50th Annual Forum*, Washington, DC, May 11–13, 1994.
9. Han, D., Rahn, C. D., and Smith, E. C., "Higher Harmonic Pitch Link Loads Reduction Using Fluidlastic Isolators," *Proceedings of the Institution of Mechanical Engineers, Part G: Journal of Aerospace Engineering*, February 2013.
10. Scarborough, L. H. III, et al. "Impedance Tailored Fluidic Pitch Links for Passive Hub Vibration Control and Improved Rotor Efficiency", *the Fifth Decennial AHS Aeromechanics Specialists' Conference*, San Francisco, California, January 22– 24, 2014.
11. Jolly, M. R. and Margolis, D. L., "Assessing the Potential for Energy Regeneration in Dynamic Subsystems," *Journal of Dynamic Systems, Measurement, and Control*, Vol. 119, (2), 1997, pp. 265–270.
12. Tauzsig, L., "Numerical Detection and Characterization of Blade Vortex Interactions Using a Free Wake Analysis," M.S. Thesis, Department of Aerospace Engineering, The Pennsylvania State University, 1998.
13. Bagai, A., "Contributions to the Mathematical Modeling of Rotor Flow-Fields Using a Pseudo-Implicit Free-Wake Analysis," Ph.D. Dissertation, Department of Aerospace Engineering, University of Maryland, 1995.
14. Johnson, W., "Self-Tuning Regulators for Multicyclic Control of Helicopter Vibration," NASA TP 1996, March 1982.
15. Sekula, M., "Helicopter Vibration Reduction Using Steady Fixed-System Auxiliary Moments and Forces," Thesis, The Pennsylvania State University, 2002.
16. Zhang, J., "Active-Passive Hybrid Optimization of Rotor Blades with Trailing Edge Flaps," Thesis, the Pennsylvania State University, 2001.

in this paper, to publish it as part of their paper. The authors confirm that they give permission, or have obtained permission from the copyright holder of this paper, for the publication and distribution of this paper as part of the ERF2014 proceedings or as individual offprints from the proceedings and for inclusion in a freely accessible web-based repository.

COPYRIGHT STATEMENT

The authors confirm that they, and/or their company or organization, hold copyright on all of the original material included in this paper. The authors also confirm that they have obtained permission, from the copyright holder of any third party material included